Resonance Raman Scattering by the Green Fluorescent Protein and an Analogue of Its Chromophore[⊥]

Peter Schellenberg,[‡,§] Ethan Johnson,[‡] Anthony P. Esposito,[†] Philip J. Reid,[†] and William W. Parson*[,‡]

Departments of Biochemistry and Chemistry, University of Washington, Seattle, Washington

Received: December 31, 2000; In Final Form: March 8, 2001

To examine the protonation state and excitation dynamics of green fluorescent protein (GFP), the electronic, resonance Raman, and Fourier transform infrared spectra of GFP were compared to the corresponding spectra of an analogue of the GFP chromophore (4-hydroxybenzylidene-2,3-dimethyl-imidazolinone, HBDI). Spectra were measured with GFP in both H_2O and D_2O and with HBDI in ordinary or deuterated ethanol under neutral, acidic, or basic conditions. The vibrational transitions were assigned with the aid of ab initio calculations using density functional theory methods. The results indicate that the main absorption band of GFP at 400 nm represents the neutral chromophore and the minor band at 475 nm represents the anion. The resonance Raman spectra of both GFP and neutral HBDI are dominated by a band in the region of 1565 cm^{-1}. We assign this band to the "C═N stretch" mode, which involves stretching of the imidazolinone C═N bond and the central C═C bond of the chromophore. The absence of resonance Raman intensity along any coordinates having substantial phenolic OH stretching character indicates that stretching of the O−H bond is not coupled strongly to the optical transition. However, substantial differences are observed between the resonance Raman spectra of GFP and HBDI, suggesting that the protein does influence the structural evolution of the excited state.

Green fluorescent protein (GFP), which serves as an energy acceptor and emitter for bioluminescence in the sea pansy *Renilla reniformis* and the jellyfish *Aequorea victoria*, is the subject of much recent interest because of its applications in molecular biology and biochemistry.[1] Most of these applications take advantage of the fact that the highly fluorescent chromophore assembles spontaneously by cyclodehydration and oxidation of the tripeptide Ser−Tyr−Gly in the nascent apoprotein.[2−5] Because formation of the chromophore requires no cofactors or substrates other than oxygen, specific fluorescent labels for proteins in living organisms can be constructed by fusing the GFP gene with genes for other proteins of interest. Mutations of GFP have led to forms with blue and yellow emission, providing tools for studies of intermolecular distances by resonance energy transfer.[4,6−10] The recent discovery of red fluorescent proteins similar to GFP in nonbioluminescent organisms has extended the spectral range even further.[11,12]

The structures of wild-type GFP from *A. victoria* and several mutant proteins have been elucidated by X-ray crystallography.[8,13−16] In addition to being linked to the protein by two covalent bonds, the chromophore participates in a network of hydrogen bonds to the surrounding protein cage. Because mutations can alter the spectral and photodynamic properties of GFP, it is clear that the protein plays a crucial part in the chromophore photophysics. At room temperature, the absorption spectrum of wild-type GFP has peaks near 400 and 475 nm, which differ in their relative heights in the proteins from *Aequorea* and *Renilla*. The relative strengths of the two bands can be influenced by mutations near the chromophore, and the band intensities depend on temperature, solvent, and, in some mutants, pH. Denaturation of the *Aequorea* and *Renilla* proteins, however, yields identical chromophores.[2,17] The spectrum of the unfolded protein depends strongly on the pH, suggesting that the two peaks represent different protonation states of the chromophore.

Time-resolved absorption and fluorescence measurements in H_2O and D_2O have confirmed that the chromophore in GFP has at least two interconvertable protonation states,[18,19] which now are commonly referred to as states A and B. The 400-nm absorption band is assigned to A, which predominates in wild-type GFP under most conditions, and the 475-nm band to B. Upon photoexcitation of A, the excited chromophore transfers a proton to an acceptor in the protein or a bound water molecule, forming a transient intermediate (I*) that emits strongly in the region of 500 nm.[18,19] Following deexcitation to the ground electronic state (I), the system usually returns to A but can branch to B with a low quantum yield. The transition from A* to I* exhibits distributed kinetics with major time constants in the range of 3−10 ps at room temperature and is slowed by a factor of 3 to 5 in D_2O.

Several studies have addressed the electronic structures of the A and B forms of GFP. Although most investigators have considered the chromophore to be uncharged in state A and anionic in B,[15,18−22] these assignments remain controversial. Voityuk et al.[23,24] have concluded from quantum calculations

[†] Department of Chemistry, Box 351700, University of Washington, Seattle, WA 98195-1700.

[‡] Department of Biochemistry, Box 357350, University of Washington, Seattle, WA 98195-7350.

[§] Current Address: Institut für Physikalische & Theoretische Chemie, Technische Universität München, Lichtenbergstr. 4, D-85748 Garching, Germany.

* To whom correspondence should be sent.

[⊥] Abbreviations: DFT, density functional theory; EtOH, ethanol; EtOD, CH_3CH_2OD; FTIR, Fourier transform infrared; GFP, green fluorescent protein; HBDI, 4-hydroxybenzylidene-2,3-dimethyl-imidazolinone; HBMIA, ethyl 4-hydroxybenzylidene-2-methyl-imidazolinone-3-acetate.

10.1021/jp0046243 CCC: $20.00
Published on Web 05/08/2001

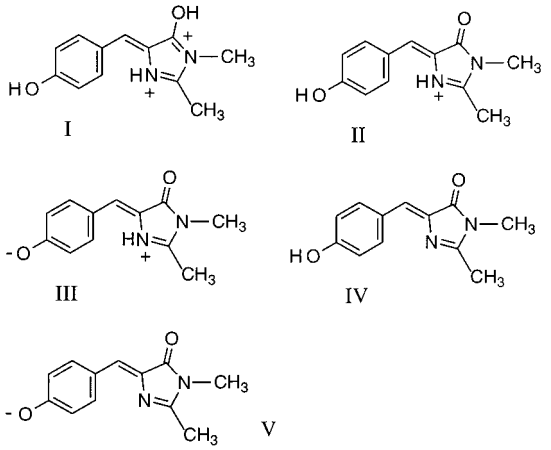

Figure 1. Valence-bond structures of 4-hydroxybenzylidene-2,3-dimethyl-imidazolinone (HBDI) in various protonation states: (I) dication, (II) cation, (III) zwitterion, (IV) neutral, and (V) anion.

of the electronic absorption spectrum that the chromophore in state A is protonated on N1 of the imidazolinone ring, making it cationic, while the chromophore in B is zwitterionic (see Figure 1). El Yazal et al.[25] have proposed that an equilibrium mixture of the uncharged and zwitterionic species predominates in the pH range of 1.1−9.4 and that the chromophore becomes cationic below pH 1.1 and anionic above 9.4. Molecular dynamics studies that considered possible cis−trans isomerization of the chromophore predicted the formation of a zwitterion as a ground-state intermediate,[26] and a zwitterion was invoked to explain the blinking behavior of GFP in single-molecule fluorescence measurements.[26−28]

The nature of state I also is currently unclear. Although conversion of I to B probably involves structural changes of the protein to stabilize an altered distribution of charge in the chromophore,[15] hole-burning and low-temperature absorption measurements indicate that I can be formed as a stable photoproduct at low temperature in wild-type GFP.[29] I also appears to be present in thermal equilibrium with B at high temperature,[29] and it has been proposed that a state similar to I is the resting state in some GFP mutants.[30,31] Recently, evidence for an even more complex pattern of photoproducts has been obtained.[32] This complex behavior seems likely to reflect variations in the arrangement of hydrogen bonds between the chromophore and the protein.[33]

Vibrational spectroscopy is often the method of choice for ascertaining the protonation and conformational states of molecules. However, the application of infrared spectroscopy is challenging in that special means have to be employed to resolve vibrational bands of the GFP chromophore in the presence of strong IR absorption by the protein. Nevertheless, Van Thor et al.[20] have used difference-FTIR spectroscopy to examine the changes in vibrational structure that accompany transformation of GFP from the A to the B form. Comparisons with the spectra of several model systems favored the view that conversion of the chromophore from form A to B involves deprotonation rather than cis−trans isomerization.

Bell et al.[21] have recently used pre-resonance Raman spectroscopy to explore the protonation state of GFP. Measurements of the spectra of a model chromophore (ethyl 4-hydroxybenzylidene-2-methyl-imidazolinone-3-acetate, HBMIA) as a function of pH supported the assignment of state A to the uncharged chromophore. The authors also found a correlation between the electronic absorption maximum and the frequency of a Raman transition in the region of 1610 to 1655 cm^{-1}.

In a previous paper, we presented IR, Raman, and resonance Raman spectra of the model chromophore 4-hydroxybenzylidene-2,3-dimethyl-imidazolinone (HBDI, Figure 1).[34] The dominant transitions were assigned with the aid of density-functional theory (DFT) calculations. Here, we expand on this earlier work by comparing resonance Raman spectra of GFP with spectra of HBDI in various ionization states and in protonated and deuterated solvents. Enhancement of Raman scattering by vibrational modes that are coupled to the electronic excitation emphasizes Raman bands of the chromophore relative to background scattering by the protein and solvent. In addition to yielding information on a chromophore's vibrational frequencies, resonance Raman spectra can provide insight into the shape of the potential energy surface of the excited state.[35,36] The vibrational modes that are enhanced most strongly are those for which the excited-state surface is shifted significantly with respect to the ground state. We find for GFP that the vibrational mode that is coupled most strongly to the optical excitation involves stretching of the chromophore's C═N and C═C bonds, with little contribution from stretching of the phenolic O−H bond. Comparison of the resonance Raman spectra of GFP and the chromophore in solution demonstrates substantial differences in transition intensity, suggesting that the protein modifies the excited-state potential energy surface of the chromophore, potentially to facilitate proton transfer.

Materials and Methods

GFP was prepared by using a histidine-tagged wild-type GFP vector from Clontech (p6xHis-GFP, Genbank accession number U89936). The vector was transformed into competent DH5α *Escherichia coli*, and the cells were grown in LB-medium[37] in 10-L fermenters at 25°. Expression of GFP was induced with 0.8 mM isopropylthiogalactoside, and cells were harvested by centrifugation 24 h later. The cells were resuspended in buffer (20 mM Tris HCl, pH 8, 100 mM NaCl) and broken in a French press in the presence of DNAase. The membrane fraction and unbroken cells were pelleted, and GFP was purified from the supernatant on a Co column (Clontech). Loading of the column could be followed easily due to the contrasting green color of GFP. Columns were washed and eluted with 50 mM imidazole buffer (pH 8). Solutions of GFP in 20 mM Tris buffer (pH 8) and 100 mM NaCl were used for study. For the Raman spectra obtained with 368.9-nm excitation (see below), the solutions also retained 50 mM imidazole from the purification procedure. For the spectra obtained with 354.7-nm excitation, the imidazole was removed by dialysis against 20 mM Tris HCl (pH 8). Deuterated GFP was prepared by concentrating the aqueous solution by pressurized dialysis and rediluting with D_2O containing 20 mM Tris HCl (pH 8). This procedure was repeated 4 to 5 times, after which the sample was stored in a D_2O for at least 24 h before use.

The GFP chromophore analogue HBDI was synthesized as described by Kojima et al.[38] and recrystallized from ethanol/chloroform (10:2). Authenticity and purity were checked by NMR.[34] Acidic solutions of HBDI in ethanol (EtOH) were prepared by adding 12 M HCl to give a final concentration of 0.6 M HCl, and basic solutions were prepared by adding 10 M NaOH to give 0.6 M NaOH.

Electronic and FTIR absorption spectra were measured as described.[34] Resonance Raman spectra were measured using excitation wavelengths of 368.9 and 354.7 nm, obtained from the hydrogen-shifted second and third harmonic output of a Nd:YAG laser (Spectra Physics, GCR-170) operating at 30 Hz. The incident light was focused onto the sample by a lens with a

75-mm focal length and a 135° backscattering geometry was employed. The scattered light was collected using standard UV-quality lenses, delivered to a 0.75-m spectrograph (Acton) with a 1200-groove/mm classically ruled grating and a polarization scrambler at the entrance and detected using an 1100 × 330 pixel, back-thinned, liquid-nitrogen cooled CCD detector (Princeton Instruments). The spectral resolution was approximately 8 cm^{-1}. All spectra were corrected for the wavelength-dependent sensitivity of the spectrometer, as measured with a calibrated quartz−tungsten−halogen lamp (Oriel).

To minimize accumulation of photoproducts, the GFP solution was flowed through a square-walled glass capillary with sapphire windows for beam entry and exit. The flow rates were sufficient to replenish the photoexcited sample volume between pulses. Resonance Raman spectra of HBDI were obtained by focusing the incident light onto a thin-film, wire-guided jet of solutions in ethanol. The dependence of the Raman scattering on incident power was measured at 368.9 nm and was found to be linear up to 30 mJ/pulse for GFP and up to 50 mJ/pulse for HBDI. Incident pulse energies were kept below these levels at 368.9 nm and were adjusted at 354.7 nm with reference to the absorption cross section to maintain the same steady-state rate of excitation. The data reported here were obtained with integration times of 120 min for GFP and 60 min for HBDI. Electronic absorption spectra were measured before and after acquiring the Raman data to check for irreversible changes in the samples, and no significant changes in the spectra were seen.

The strong fluorescence from GFP contributes a substantial background to the resonance Raman spectra. The fluorescence quantum yield of the chromophore in GFP is approximately 80%.[17,39] Fortunately, the shift between excitation of state A and the dominant emission peak is quite large. When GFP was excited in the blue wing of the absorption spectrum, the intensity of the strongest Raman peak was approximately equal to the fluorescence background. Although the Raman peaks at other wavelengths were 5 to 10 times weaker, extensive signal averaging made the signal-to-noise ratio for these transitions acceptable. The fluorescence background was subtracted from the spectra after fitting to a spline function. The much weaker fluorescence from HBDI was removed in the same manner.

Intensities of Raman peaks were determined by a nonlinear, least-squares fit of the spectrum to a sum of Lorentzian peaks convolved with a Gaussian instrument response and a linear background. The relative Raman intensities reported here are considered accurate to ± 9%.

Methods employed in measuring the IR absorption spectrum of the chromophore have been reported elsewhere.[34] To measure the IR spectrum of the anionic form of the chromophore, HBDI was dissolved in alkaline methanol, the solvent was evaporated, and the solid HBDI was compacted in a KBr pellet. This preparation was repeated with varying ratios of KOH to HBDI in the solvent to check for adverse effects of drying the sample under strongly alkaline conditions.

Normal-mode calculations for HBDI in various protonation states were done as described previously,[34] using the program Gaussian 98.[40] The DFT hybrid method B3LYP with basis set 6-31G* was used for both geometry optimization and calculating the vibrational frequencies. This method has been shown to give vibrational frequencies with the least scattering around the experimental values for a large number of vibrational modes in small molecules.[41−43] The recommended scaling factor[41,42] of 0.9614 for frequencies calculated by B3LYP/6-31G* was applied to the results presented here. In previous work,[34] we evaluated Hartree−Fock and DFT methods with basis sets of higher complexity and found B3LYP/6-31G* to work well for calculating vibrational frequencies and relative IR and Raman intensities of the neutral form of HBDI. The vibrational modes were visualized with the programs Molden[44] and HyperChem.[45]

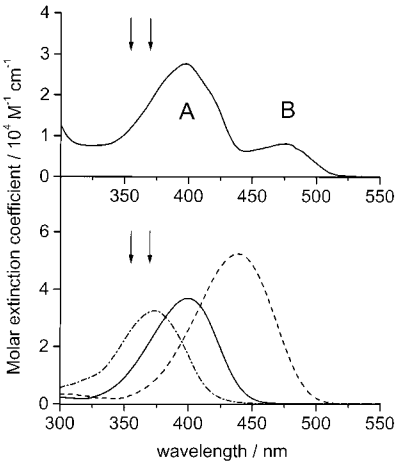

Figure 2. (Top) Absorption spectrum of GFP in 20 mM Tris HCl buffer (pH 8) and 100 mM NaCl. The ordinate is scaled using the molar extinction coefficient given by Ward.[53] The absorption bands attributed to the A and B forms of the chromophore are labeled. (Bottom) Absorption spectra of the GFP-analogue chromophore HBDI in neutral (•−•), acidic (—), and basic (- - -) EtOH. The vertical arrows indicate the excitation wavelengths used in the Raman measurements (368.9 and 354.7 nm).

Results and Discussion

Electronic absorption spectra of GFP and an analogue of its chromophore (HBDI) are shown in Figure 2. As discussed above, the absorption bands of GFP at 398 and 476 nm have been assigned to the A and B protonation states of the chromophore, and there is general agreement that the chromophore has one less proton in the state B. Most investigators[15,18−21] have taken A to be the neutral chromophore and B the anion, but others[23,24] have suggested that A is the cation and B is the zwitterion (see Figure 1). To explore this issue, we investigated the pH dependence of the absorption and Raman spectra of HBDI. As Figure 2 shows, the neutral form of HBDI in ethanol has an absorption maximum at 373 nm, while the peak for the basic species is red-shifted by 66 nm (4030 cm^{-1}) to 439 nm. The acidic form also is red-shifted but only by 27 nm (1810 cm^{-1}). The red shift under alkaline conditions is comparable to the 78-nm (4120 cm^{-1}) difference between the absorption maxima of the deprotonated (B) and protonated (A) forms of GFP. In water, the absorption maxima of HBDI shift to the blue by 3 to 7 nm (not shown). Niwa et al.[46] and Bell et al.[21] have described similar spectral shifts for another analogue of the GFP chromophore (HBMIA) in a variety of solvents.

Resonance Raman spectra of GFP in H_2O are shown in Figure 3. The spectra were obtained by excitation on the blue edge of the major absorption band of the A form of the protein at pH 8.0. The resonance Raman spectra are relatively sparse and are dominated by a single peak at 1565 cm^{-1}. Weaker bands with intensities less than 10% that of the dominant band are observed at both higher and lower energies (Table 1). The transition at 1565 cm^{-1} corresponds to a mode that is dominated by stretching of the imidazolinone C═N bond (see below and ref 34). We will refer to this mode as the "C═N stretch" for convenience; however, the mode also involves stretching of the C═C bond between the phenol and imidazolinone rings along with smaller in-plane motions of other atoms. Figure 3

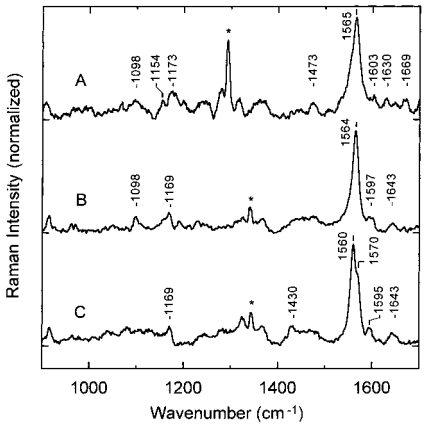

Figure 3. (A) Resonance Raman spectrum of GFP in aqueous 20 mM Tris HCl buffer (pH 8), 100 mM NaCl and 50 mM imidazole, measured with excitation at 368.9 nm. (B) Same as panel A except that the imidazole was removed from the buffer and excitation was at 354.7 nm. (C) Same as panel B except that H_2O was replaced by D_2O. Features marked with asterisks are background artifacts that also were seen in the absence of GFP.

TABLE 1: Resonance Raman Transitions of GFP[a]

	relative intensity[a]	
frequency (cm^{-1})	H_2O	D_2O
1643	0.07	0.14
1597	0.04	
1595		0.09
1570		0.18
1564	1.00	
1560		1.00
1430		0.16
1169	0.07	0.07
1098	0.08	

[a] Integrated intensities of resonance Raman scattering relative to the main band at 1564 cm^{-1} in H_2O and 1560 cm^{-1} in D_2O. The data were obtained by excitation at 354.7 nm.

demonstrates that excitation at either 368.9 or 354.7 nm produces Raman spectra with similar relative intensities, as would be expected considering the broad, unstructured nature of the absorption band.[29,35,47] However, 1565-cm^{-1} band was broader with excitation at 368.9 nm, possibly because exciting at longer wavelengths results in larger contributions from the B-form of the chromophore, which is present as a minority component.

Resonance Raman spectra of HBDI were measured as a function of the acidity of the solvent. The results are presented in Figure 4. HBDI has a much lower fluorescence yield than GFP, providing a significant improvement in the signal-to-noise ratio. The decreased fluorescence likely results from a radiationless decay channel involving rotation around the central C═C bond, which is available to HBDI but presumably is blocked by the protein in GFP.[26,46] This interpretation is supported by a strong increase of fluorescence when the chromophore is cooled below the glass-transition temperature of the solvent[38,46] or is embedded in poly(vinyl alcohol) (E. Meyer and P. Schellenberg, unpublished). As described previously,[34] the resonance Raman spectrum of neutral HBDI (Figure 4C) is dominated by the C═N stretch band near 1560 cm^{-1}; however, many other transitions throughout the fingerprint region are observed as well. Bands at 1641, 1603, 1446, and 1173 cm^{-1} are evident and correspond to bands seen in GFP, but the intensities of these transitions relative to the C═N stretch are two to three times stronger in HBDI than in GFP.

The spectrum presented in Figure 4A was recorded in acidic EtOH, where HBDI exists mainly as the monocation. (The pK_a for protonation of the imidazolinone N is 1.8 in both denatured GFP and the closely related analogue HBMIA.[9,21]) The dominant resonance Raman band shifts to higher energy by 17 cm^{-1} in the cation, as would be expected for a mode that involves stretching of the imidazolinone C═N bond. The band at 1446 cm^{-1} in neutral HBDI, which has been assigned to a "C−N stretch" mode of the imidazolinone ring,[34] also is strongly attenuated or shifted in the cation. The "C═C stretch" and "phenol1" modes at 1641 and 1603 cm^{-1}, which involve mainly other parts of the molecule,[34] are less affected, shifting by only 7 and −6 cm^{-1}, respectively.

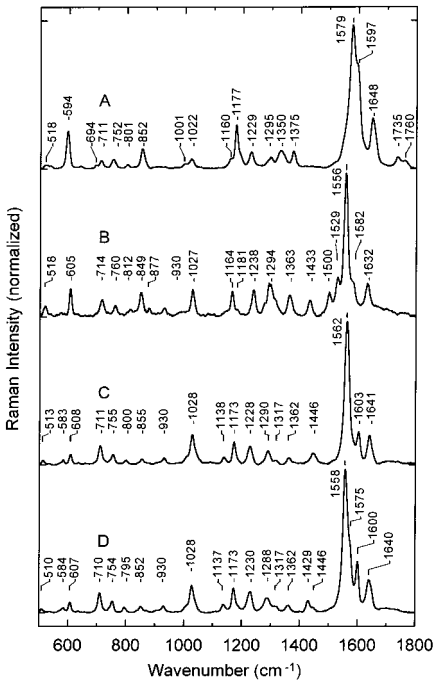

Figure 4. Resonance Raman spectra of HBDI measured with excitation at 368.9 nm in acidic EtOH (A), basic EtOH (B), neutral EtOH (C), or neutral EtOD (D).

Figure 4B shows the resonance Raman spectrum of HBDI in basic EtOH, where HBDI exists mainly as the anion. (The pK_a for dissociation of the phenolic proton in HBMIA is 8.2.[21]) A Raman band corresponding to the phenol1 transition of neutral HBDI now is seen at 1582 cm^{-1}, shifted by −21 cm^{-1} from its position in neutral HBDI. By contrast, the dominant C═N stretch transition shifts by only −6 cm^{-1}. The "phenol3" and "phenol4" bands[34] in the region between 1530 and 1500 cm^{-1} become more prominent in the anion.

Resonance Raman spectra of GFP in D_2O and of neutral HBDI in EtOD are shown in Figures 3C and 4D, respectively. While GFP in H_2O has a single peak at 1564 cm^{-1}, two transitions are seen in this frequency region in D_2O, with the peak shifting to 1560 cm^{-1} and a shoulder appearing at 1570 cm^{-1}. A similar shifting and splitting of the major band occurs with HBDI in EtOD, where the peak moves from 1562 to 1558 cm^{-1} and a shoulder appears at 1575 cm^{-1}. The shoulder has been assigned to a vibrational mode ("phenol2") that involves the phenol ring.[34]

The FTIR absorption spectrum of neutral HBDI was described in our previous work.[34] The frequencies and relative intensities of the FTIR bands of the HBDI anion are given in Table 2. The anion has IR bands at 1589, 1497, and 1139 cm^{-1}, which probably correspond to bands at 1580, 1497, and 1147 cm^{-1} that appear as positive features in the B − A FTIR difference spectrum for GFP as measured by Van Thor et al.[20] The FTIR

TABLE 2: Infrared Transitions of Anionic HBDI in KBr[a]

frequency (cm^{-1})	relative intensity[a]
1665	0.30
1639	0.47
1589	1.00
1560	0.32
1497	0.82
1445	0.48
1296	0.90
1262	0.47
1165	0.52
1139	0.60
1031	0.50
1000	0.18
933	0.07
906	0.08
849	0.38
805/812	0.33
764	0.25
712	0.11
608	0.32
518	0.33

[a] Integrated intensities of infrared absorption bands relative to the band at 1589 cm^{-1}.

spectrum of the HBDI anion also has a strong band at 1296 cm^{-1}, which probably corresponds to an FTIR band of neutral HBDI at 1277−1282 cm^{-1}.[34] The B − A difference spectrum shows what appears to be a shift to higher frequencies in this region.[20] The relatively weak FTIR line of the HBDI anion at 1560 cm^{-1} (Table 2) probably corresponds to the strong Raman line at 1556 cm^{-1}. The small discrepancy in transition frequencies could reflect the experimental difficulty of resolving the FTIR line in the presence of the strong line at 1589 cm^{-1}, which probably corresponds to the weak feature at 1582 cm^{-1} in the resonance Raman spectrum.

To assign and visualize the vibrational modes of HBDI as a function of protonation state, we have carried out ab initio calculations using density functional theory (DFT). Figure 5 shows the calculated frequencies and intensities of the Raman and IR bands of HBDI in five different protonation states, and Figure 6 shows the results of similar calculations when the exchangeable hydrogen atoms were replaced by deuterium. Because the Raman intensities calculated by DFT are for off-resonance Raman scattering, the relative intensities predicted by DFT are expected to differ from the relative intensities of the measured resonance Raman bands. The calculated intensities do, however, provide a measure of whether a particular mode will be IR- or Raman-active. It is important to note also that deuteration or changing the ionization state of HBDI modifies the character of the HBDI normal modes. One indication of such a modification is that the strongest transition of the neutral species is highly Raman-active and only weakly IR-active, whereas the strongest transitions of the cationic and anionic species are strongly IR-active and weakly Raman-active. Figure 7 shows structural drawings of the C═N stretch and phenol2 modes for the neutral chromophore with H or D on the phenolic oxygen atom. Structural drawings of additional vibrational modes of the neutral chromophore with H at this position have been presented previously.[34]

The C═O stretch mode serves as a useful reference point for comparing the calculated and measured vibrational spectra. This mode can be identified by its location as the highest-frequency vibrational mode in the fingerprint region and by its relatively high calculated IR intensity combined with a virtual absence of Raman activity. The C═O stretch transition is calculated to occur between 1670 and 1780 cm^{-1} in all

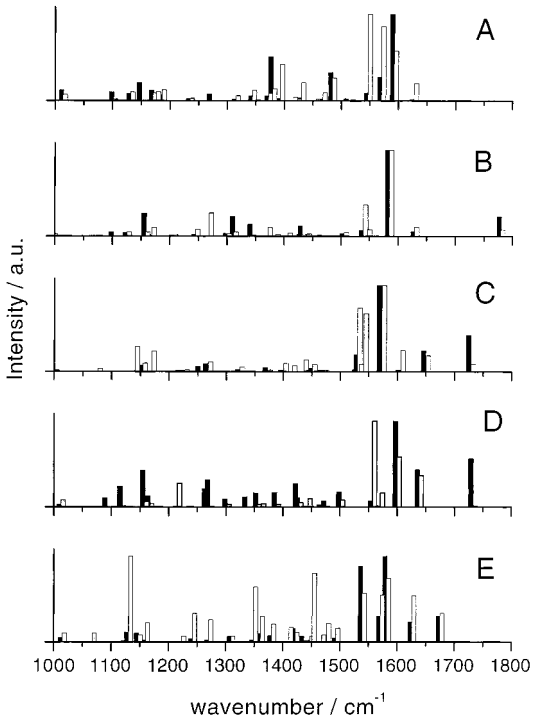

Figure 5. Calculated Raman (gray bars) and IR (black) spectra of HBDI in various protonation states: (A) dication, (B) cation, (C) zwitterion, (D) neutral, and (E) anion. The spectra were calculated with B3LYP/6-31G* and the wavenumbers were corrected by a factor of 0.9614. The bars for IR and Raman transitions are shifted by half the bar width to lower and higher energy, respectively. The heights of the bars are normalized to the strongest transition in each spectrum.

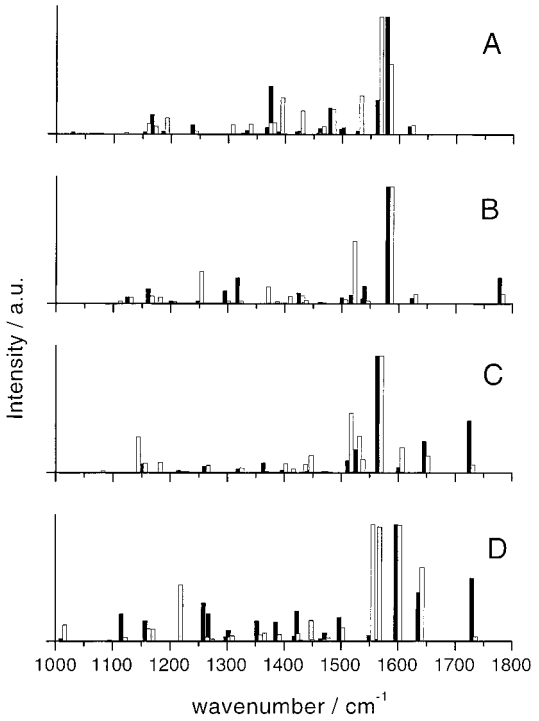

Figure 6. Calculated Raman (gray) and IR (black) spectra of deuterated HBDI in various protonation states: (A) dication, (B) cation, (C) zwitterion, and (D) neutral. Only the proton(s) bound to oxygen or nitrogen atoms were replaced by deuterium. The heights of the bars are normalized to the strongest transition in each spectrum and the bars are shifted as in Figure 5.

protonation states other than the dication, where the C−O bond order and charges are severely perturbed (see Figure 5). Corresponding lines with strong FTIR intensity and little or no

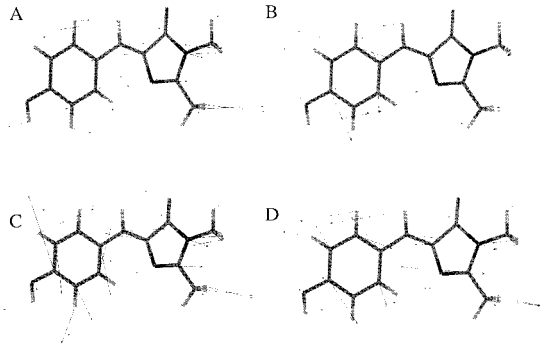

Figure 7. HyperChem representations of the C═N stretch (A and C) and phenol2 (B and D) normal modes of neutral HBDI with H (A and B) or D (C and D) on the phenolic oxygen. The calculated transition energies, after scaling as described in the text, were 1558, 1572, 1553, and 1565 cm^{-1} for A, B, C, and D, respectively.

resonance Raman strength are seen experimentally at 1677 cm^{-1} with HBDI in neutral EtOH[34] and at 1665 cm^{-1} in basic EtOH (Table 2). The calculated C═O stretching frequency for the anion agrees well with the measured value, while that for the neutral species is considerably higher than observed. At least part of the discrepancy in the case of neutral HBDI probably reflects hydrogen bonding of the oxygen atom, which would shift the C═O stretching to lower frequencies. In GFP, this oxygen forms hydrogen bonds to the side chains of both Arg-96 and Gln-94.[15] We therefore calculated the Raman and IR spectra of a model of neutral HBDI with a molecule of water near the carbonyl oxygen atom. The calculated spectra are available in the Supporting Information (Figure 1S). Including a hydrogen-bonded water near the oxygen decreased the C═O stretching frequency in neutral HBDI by 26 cm^{-1}. For comparison, we also examined a model with a hydrogen-bonded water molecule next to the phenolic OH group and a second alongside the imidazolinone nitrogen. Hydrogen bonding at these positions had very little effect on the calculated C═O stretching frequency and also had only very small effects on the other vibrational modes. The major Raman transition shifted to lower energy by 6 cm^{-1}, and its relative intensity increased by about 10%. (It should be noted that the calculated frequency of the C═O stretching mode is comparatively sensitive to the size of the basis set, and thus may be less reliable than the frequencies of the other major modes. Calculations with the B3LYP/6-31++G* basis lowered the frequency of the C═O stretch by 30 cm^{-1} relative to the results obtained with B3LYP/6-31G*, while lowering most of the other vibrations by only 5 to 10 cm^{-1}.)

Comparisons of the calculated and measured vibrational spectra provide strong evidence that the A form of GFP contains the neutral chromophore and that the B form therefore must contain the anion. In particular, the neutral species is calculated to have a weak Raman line near 1570 cm^{-1} that gains intensity on deuteration (compare Figures 5D and 6D). The enhancement of this "phenol2" mode probably accounts for the splitting of the 1565-cm^{-1} Raman line of GFP in D_2O (Figure 3C) and of the corresponding line of HBDI in EtOD (Figure 4D), as discussed previously for HBDI.[34] This spectral evolution is not predicted to occur on deuteration of the cationic chromophore (see Figures 5B and 6B). Conversely, the cation is predicted to have a strong Raman line near 1590 cm^{-1} (see Figure 5B), which probably corresponds to the major Raman peak of HBDI in acidic EtOH (Figure 4A). The corresponding Raman band in A-form GFP is relatively weak (Figure 3A,B).

The resonance Raman spectra of HBDI are qualitatively similar to the pre-resonance Raman spectra of HBMIA described by Bell et al.;[21] however, some differences are observed. For example, in the region between 1070 and 1100 cm^{-1}, Bell et al. found Raman bands at 1098, 1095, and 1077 cm^{-1} for the neutral, anionic, and cationic chromophore, respectively. We found no significant resonance Raman scattering in this region (Figure 4) and also no resolved FTIR absorption.[34] However, the resonance Raman spectra of GFP show weak but possibly significant scattering at 1098 cm^{-1} (Figure 3), as do the preresonance Raman spectra of wild-type and S65T GFP measured by Bell et al. The Raman peak in the region of 1640 cm^{-1}, which Bell et al. found to shift in concert with the electronic absorption maximum, is probably the C═C stretching mode.[34]

The major modes in the resonance Raman spectrum should correspond to vibrational progressions that contribute to the absorption and fluorescence spectra. Recent low-temperature and hole-burning spectroscopic studies have pointed to vibrational energies of 570 and 1440 cm^{-1} for the A form of the chromophore in GFP and 765 and 1510 cm^{-1} for the B form.[29] Considering the limited resolution of vibrational structure in the absorption spectrum, particularly in the A form,[18,29] the vibrational modes at 1440 and 1510 cm^{-1} could possibly correspond to the strong Raman mode 1565 cm^{-1}.

The resonance Raman spectra provide some insight into how the protein modifies the energy surface of the chromophore's excited state. Although a single vibrational transition dominates the resonance Raman spectra of both GFP and HBDI in solution, the relative intensities of the other Raman lines are strongly suppressed in the protein as compared to the free chromophore. This is particularly true in the region around 1000 cm^{-1}. The resonance Raman scattering intensity of a given mode depends on the displacement of the excited-state potential surface relative to the energy minimum of the ground state and on the slope of the excited-state surface at the equilibrium geometry of the ground state.[35,36] The observed resonance Raman spectra thus suggest that the environment in the protein favors distortion of the excited chromophore along the vibrational coordinate associated with the 1560-cm^{-1} mode, which is dominated by stretching of the C═N and C═C bonds.[34] The vibration that is coupled most strongly to the electronic excitation thus modulates the length of the chromophore but has little direct effect on the length of the phenolic O−H bond, where proton dissociation ultimately occurs. This conclusion is in accord with studies of excited-state proton transfer in several other chromophores, where delocalized in-plane motions also appear to dominate the initial movement out of the Franck−Condon region.[48−52] As Figure 7 illustrates, however, replacing the exchangeable H atom of the OH group by D modifies the compositions of some of the normal modes. The phenol2 mode, in particular, acquires stronger motion of the imidazolinone C═N atoms (compare Figure 7B and D), while the C═N stretch mode gains motions of atoms in the phenol ring (compare Figure 7A and C). This rearrangement of the normal modes could bear on the effect of D_2O on the dynamics of the excited state in GFP.[18]

Several investigators have discussed the possibility of rapid dynamics around the central C═C bond of GFP.[26,46] Although the X-ray structure shows unambiguously that the chromophore in resting (A-form) GFP is the cis isomer, greater conformational flexibility is available to the free chromophore. For example, the rapid internal conversion that competes with fluorescence in solution could possibly reflect cis-trans isomerization.[46] Therefore, for completeness, we also calculated the vibrational modes of the trans isomer of the chromophore. The calculated vibrational frequencies and intensities of the major IR and

Raman bands and the effects of deuteration are similar to those calculated for the cis isomer and do not provide a firm basis for determining which isomer is present in solution (results not shown). The calculated electronic absorption spectra of the cis and trans isomers also are similar. The major difference in the vibrational spectra is in the C═O stretching frequency, which moves to lower energy by about 30 cm^{-1} in the trans isomer. The observed frequency of this mode is not diagnostic because, as mentioned above, the calculated frequency is sensitive to hydrogen bonding and to the choice of basis set. However, the DFT calculations gave the cis isomer of HBDI a lower total energy by about 3.5 kcal/mol as compared to the trans isomer, suggesting that the cis isomer would predominate in nonpolar solvents.

Acknowledgment. We thank Craig Beeson, Michael Hart, and Bart Kahr for their help in the synthesis of HBDI, the National Science Foundation (Grant MCB-9904618) for support, and A. Voityuk, A. Kummer, M.-E. Michel-Beyerle, and V. Nagarajan for useful discussions. P.J.R. is a Cottrell Fellow of the Research Corporation and an Alfred P. Sloan Fellow.

Supporting Information Available: Calculated Raman and IR spectra of neutral HBDI with H-bonds to the phenolic OH and the imidazolinone NH, with a single H-bond to the imidazolinone C═O and with no H-bonds. This material is available free of charge via the Internet at http://pubs.acs.org.

References and Notes

(1) Tsien, R. Y. *Annu. Rev. Biochem.* **1998**, *67*, 509.
(2) Ward, W. W.; Bokman, S. H. *Biochem.* **1982**, *21*, 4535.
(3) Prasher, D. C.; Eckenrode, V. K.; Ward, W. W. *Gene* **1992**, *111*, 229.
(4) Heim, R.; Prasher, D. C.; Tsien, R. Y. *Proc. Natl. Acad. Sci. U.S.A.* **1994**, *91*, 12501.
(5) Nishiuchi, Y.; Inui, T.; Nishio, H.; Bodi, J.; Kimura, T.; Tsuji, F. I.; Sakakibara, S. *Proc. Natl. Acad. Sci. U.S.A.* **1998**, *95*, 13549.
(6) Cormack, B. P.; Valdivia, R. H.; Falkow, S. *Gene* **1996**, *173*, 33.
(7) Crameri, A.; Whitehorn, E. A.; Tate, E.; Stemmer, W. P. C. *Nat. Biotechnol.* **1996**, *14*, 315.
(8) Palm, G.; Zdanov, A.; Gaitanaris, G. A.; R., S.; Pavlakis, G. N.; Wlodawer, A. *Nat. Struct. Biol.* **1997**, *4*, 361.
(9) Palm, G. J.; Wlodawer, A. *Methods Enzymol.* **1999**, *302*, 378.
(10) Cubitt, A. B.; Heim, R.; Adams, S. R.; Boyd, A. E.; Gross, L. A.; Tsien, R. Y. *Trends Biochem. Sci.* **1995**, *20*, 448.
(11) Matz, M. V.; Fradkov, A. F.; Labas, Y. A.; Savitsky, A. P.; Zaraisky, A. G.; Markelov, M. L.; Lukyanov, S. A. *Nat. Biotechnol.* **1999**, *17*, 969.
(12) Lukyanov, K. A.; Fradkov, A. F.; Gurskaya, N. G.; Matz, M. V.; Labas, Y. A.; Savitsky, A. P.; Markelov, M. L.; Zaraisky, A. G.; Zhao, X. N.; Fang, Y.; Tan, W. Y.; Lukyanov, S. A. *J. Biol. Chem.* **2000**, *275*, 25879.
(13) Ormö, M.; Cubitt, A. B.; Kallio, K.; Gross, L. A.; Tsien, R. Y.; Remington, S. J. *Science* **1996**, *273*, 1392.
(14) Yang, F.; Moss, L. G.; Phillips, G. N. *Nat. Biotechnol.* **1996**, *14*, 1246.
(15) Brejc, K.; Sixma, T. K.; Kitts, P. A.; Kain, S. R.; Tsien, R. Y.; Ormo, M.; Remington, S. J. *Proc. Natl. Acad. Sci. U.S.A.* **1997**, *94*, 2306.
(16) Wachter, R. M.; King, B. A.; Heim, R.; Kallio, K.; Tsien, R. Y.; Boxer, S. G.; Remington, S. J. *Biochemistry* **1997**, *36*, 9759.
(17) Ward, W. W.; Cody, C. W.; Hart, R. C. *Photochem. Photobiol.* **1980**, *31*, 611.
(18) Chattoraj, M.; King, B. A.; Bublitz, G. U.; Boxer, S. G. *Proc. Natl. Acad. Sci. U.S.A.* **1996**, *93*, 8362.
(19) Lossau, H.; Kummer, A.; R., H.; Pöllinger-Dammer, F.; Kompa, C.; Bieser, G.; Jonsson, T.; Silva, C. M.; Yang, M. M.; Youvan, D. C.; Michel-Beyerle, M.-E. *Chem. Phys.* 1996, *213*, 1.
(20) Van Thor, J. J.; Pierik, A. J.; Nugteren-Roodzant, I.; Xie, A. H.; Hellingwerf, K. J. *Biochemistry* **1998**, *37*, 16915.
(21) Bell, A. F.; He, X.; Wachter, R. M.; Tonge, P. J. *Biochemistry* **2000**, *39*, 4423.
(22) Scharnagl, C.; Raupp-Kossmann, R.; Fischer, S. F. *Biophys. J.* **1999**, *77*, 1839.
(23) Voityuk, A. A.; Michel-Beyerle, M.-E.; Rösch, N. *Chem. Phys. Lett.* **1997**, *272*, 162.
(24) Voityuk, A. A.; Michel-Beyerle, M.-E.; Rösch, N. *Chem. Phys.* **1998**, *231*, 13.
(25) El Yazal, J.; Prendergast, F. G.; Shaw, D. E.; Pang, Y.-P. *J. Am. Chem. Soc.* **2000**, *122*, 11411.
(26) Weber, W.; Helms, V.; McCammon, J. A.; Langhoff, P. W. *Proc. Natl. Acad. Sci. U.S.A.* **1999**, *96*, 6177.
(27) Dickson, R. M.; Cubitt, A. B.; Tsien, R. Y.; Moerner, W. E. *Nature* **1997**, *388*, 355.
(28) Jung, G.; Wiehler, J.; Gohde, W.; Tittel, J.; Basché, T.; Steipe, B.; Bräuchle, C. *Bioimaging* **1998**, *6*, 54.
(29) Creemers, T. M. H.; Lock, A. J.; Subramaniam, V.; Jovin, T. M.; Volker, S. *Nat. Struct. Biol.* **1999**, *6*, 557.
(30) Kummer, A. D.; Wiehler, J.; Rehaber, H.; Kompa, C.; Steipe, B.; Michel-Beyerle, M. E. *J. Phys. Chem B* **2000**, *104*, 4791.
(31) Creemers, M. H.; Lock, A. J.; Subramaniam, V.; Jovin, T. M.; Völker, S. *Proc. Natl. Acad. Sci. U.S.A.* **2000**, *97*, 2974.
(32) Seebacher, C.; Deeg, F. W.; Bräuchle, C.; Wiehler, J.; Steipe, B. *J. Phys. Chem. B* **1999**, *103*, 7728.
(33) Stübner, M. R.; Schellenberg, P., submitted for publication, 2001.
(34) Esposito, A. P.; Schellenberg, P.; Parson, W. W.; Reid, P. J. *J. Mol. Struct.* **2001**, in press.
(35) Myers, A. B.; Mathies, R. A. Resonance Raman intensities: a probe of excited-state structure and dynamics. In *Biological Applications of Raman Spectrometry: Vol. 2. Resonance Raman Spectra of Polyenes and Aromatics*; Spiro, T. G., Ed.; John Wiley: New York, 1987; Vol. II; p 1.
(36) Myers, A. B. *J. Raman Spectrosc.* **1997**, *28*, 389.
(37) Sambrook, J.; Fritsch, E. F.; Maniatis, T.. In *Molecular Cloning: A Laboratory Manual*; Cold Spring Harbor Laboratory Press: Plainview, NY, 1989; Vol. 3; Appendix A1.
(38) Kojima, S.; Ohkawa, H.; Hirano, T.; Maki, S.; Niwa, H.; Ohashi, M.; Inouye, S.; Tsuji, F. I. *Tetrahed. Lett.* **1998**, *39*, 5239.
(39) Patterson, G. H.; Knobel, S. M.; Sharif, W. D.; Kain, S. R.; Piston, D. W. *Biophys. J.* **1997**, *73*, 2782.
(40) Frisch, M. J.; Trucks, G. W.; Schlegel, H. B.; Scuseria, G. E.; Robb, M. A.; Cheeseman, J. R.; Zakrzewski, V. G.; Montgomery, J. A. J.; Stratmann, R. E.; Burant, J. C.; Dapprich, S.; Millam, J. M.; Daniels, A. D.; Kudin, K. N.; Strain, M. C.; Farkas, O.; Tomasi, J.; Barone, V.; Cossi, M.; Cammi, R.; Mennucci, B.; Pomelli, C.; Adamo, C.; Clifford, S.; Ochterski, J.; Petersson, G. A.; Ayala, P. Y.; Cui, Q.; Morokuma, K.; Malick, D. K.; Rabuck, A. D.; Raghavachari, K.; Foresman, J. B.; Cioslowski, J.; Ortiz, J. V.; Baboul, A. G.; Stefanov, B. B.; Liu, G.; Liashenko, A.; Piskorz, P.; Komaromi, I.; Gomperts, R.; Martin, R. L.; Fox, D. J.; Keith, T.; Al-Laham, M. A.; Peng, C. Y.; Nanayakkara, A.; Gonzalez, C.; Challacombe, M.; Gill, P. M. W.; Johnson, B.; Chen, W.; Wong, M. W.; Andres, J. L.; C., G.; Head-Gordon, M.; Replogle, E. S.; Pople, J. A. Gaussian 98, Rev. A.7; Gaussian Inc.: Pittsburgh, PA, 1998.
(41) Rauhut, G.; Pulay, P. *J. Phys. Chem.* **1995**, *99*, 3093.
(42) Scott, A. P.; Radom, L. *J. Phys. Chem.* **1996**, *100*, 16502.
(43) Schettino, V.; Gervasio, F. L.; Cardini, G.; Salvi, P. R. *J. Chem. Phys.* **1999**, *110*, 3241.
(44) Schaftenaar, G.; Noordik, J. H. *J. Comput.-Aided Mol. Design* **2000**, *14*, 123.
(45) Hypercube. HyperChem Reference Manual; Hypercube, Inc.: Gainesville, FL, 1996.
(46) Niwa, H.; Inouye, S.; Hirano, T.; Matsuno, T.; Kojima, S.; Kubota, M.; Ohashi, M.; Tsuji, F. I. *Proc. Natl. Acad. Sci. U.S.A.* **1996**, *93*, 13617.
(47) Bublitz, G.; King, B.; Boxer, S. G. *J. Am. Chem. Soc.* **1998**, *120*, 9370.
(48) Peteanu, L. A.; Mathies, R. A. *J. Phys. Chem.* **1992**, *96*, 6910.
(49) Pfeiffer, M.; Lau, A.; Lenz, K.; Elsaesser, T. *Chem. Phys. Lett.* **1997**, *268*, 258.
(50) Marzocchi, M. P.; Mantini, A. R.; Casu, M.; Smulevich, G. *J. Chem. Phys.* **1998**, *108*, 534.
(51) Garavelli, M.; Negri, F.; Olivucci, M. *J. Am. Chem. Soc.* **1999**, *121*, 1023.
(52) Gonzalez-Luque, R.; Garavelli, M.; Bernardi, F.; Merchan, M.; Robb, M. A.; Olivucci, M. *Proc. Natl. Acad. Sci. U.S.A.* **2000**, *97*, 9379.
(53) Ward, W. W. In *Green Fluorescent Protein: Properties, Applications and Protocols*; Chalfie, M., Kain, S., Eds.; Wiley-Liss: New York, 1998; p 45.